Efficient internalization of TAT peptide in zwitterionic DOPC phospholipid membrane revealed by neutron diffraction

Efficient internalization of TAT peptide in zwitterionic DOPC phospholipid membrane revealed by neutron diffraction

Xiaochao Chen, Shutao Liu, Bruno Deme, Viviana Cristiglio, Drew Marquardt, Richard Weller, Pingfan Rao, Yunqiang Wang, Jeremy Bradshaw

PII: S0005-2736(17)30044-5
DOI: doi:10.1016/j.bbamem.2017.01.036
Reference: BBAMEM 82418

To appear in: *BBA - Biomembranes*

Received date: 28 November 2016
Revised date: 16 January 2017
Accepted date: 28 January 2017

Please cite this article as: Xiaochao Chen, Shutao Liu, Bruno Deme, Viviana Cristiglio, Drew Marquardt, Richard Weller, Pingfan Rao, Yunqiang Wang, Jeremy Bradshaw, Efficient internalization of TAT peptide in zwitterionic DOPC phospholipid membrane revealed by neutron diffraction, *BBA - Biomembranes* (2017), doi:10.1016/j.bbamem.2017.01.036

Efficient internalization of TAT peptide in zwitterionic DOPC phospholipid membrane revealed by neutron diffraction

Xiaochao Chen[1,2], Shutao Liu[1], Bruno Deme[3], Viviana Cristiglio[3], Drew Marquardt[4], Richard Weller[2], Pingfan Rao[1], Yunqiang Wang[1] and Jeremy Bradshaw[5]

[1] College of Biological Science and Biotechnology, Fuzhou University, 2 Xue Yuan Road, University Town 350116, Fuzhou, Fujian, P.R.C; [2] The University of Edinburgh, Medical Research Council Centre for Inflammation Research, Queens Medical Research Institute, 47 Little France Crescent, Edinburgh, EH16 4TJ, United Kingdom.; [3] Institut Laue-Langevin, 6 rue Jules Horowitz, BP 156, F-38042 Grenoble Cedex 9, France; [4] Canadian Neutron Beam Centre, National Research Council, Chalk River, ON, K0J 1P0, Canada; [5] The University of Edinburgh, Royal (Dick) School of Veterinary Studies, Easter Bush, Roslin, Midlothian, EH25 9RG, United Kingdom

Abstract

The aim of this study is to investigate the interactions between TAT peptides and a neutral DOPC bilayer by using neutron lamellar diffraction. The distribution of TAT peptides and the perturbation of water distribution across the DOPC bilayer were revealed. When compared to our previous study on an anionic DOPC/DOPS bilayer (X. Chen *et al*., Biochim Biophys Acta. 2013. 1828 (8), 1982-1988), a much deeper insertion of TAT peptides was found in the hydrophobic core of DOPC bilayer at a depth of 6.0 Å from the center of the bilayer, a position close to the double bond of fatty acyl chain. We conclude that the electrostatic attractions between the positively charged TAT peptides and the negatively charged headgroups of phospholipid are not essential for the direct translocation. Furthermore, the interactions of TAT peptides with the DOPC bilayer were found to vary in a concentration-dependent manner. A limited number of peptides first associate with the phosphate moieties on the lipid headgroups by using the guanidinium ions pairing. Then the energetically favorable water defect structures are adopted to maintain the arginine residues hydrated by drawing water molecules and lipid headgroups into the bilayer core. Such bilayer deformations consequently lead to the deep intercalation of TAT peptides into the bilayer core. Once a threshold concentration of TAT peptide in the bilayer is reached, a significant rearrangement of bilayer will happen and steady-state water pores will form.

Keywords: cell penetrating peptide; TAT peptide; neutron diffraction; phospholipid

Introduction

Since the first discovery of HIV-TAT peptide in late 1980s, a large family of short peptides capable of penetrating cell membrane without causing significant membrane defect have been specifically termed as cell penetrating peptides (CPPs) [1,2]. They are very promising transporters for intracellular delivery of various bioactive molecules with high efficiency, low cytotoxicity and low immunogenicity [3-9]. Numerous experimental studies have been established to better understand how CPPs manage to overcome the prodigious thermodynamic cost of membrane internalization [10-12]. However, the detailed mechanisms of internalization of CPPs are still controversial which depend on a great variety of aspects such as the nature and size of CPP and its cargo, the concentration used, the temperature involved, and the cell lines targeted etc [13-15]. Despite of a lot of controversy and debate, the common consensus is that both direct translocation and energy-dependent endocytosis

mechanism are involved [12,13]. While the endocytosis pathway has been generally accepted, the direct translocation across the membrane has been constantly questioned over years [13,14,16]. In terms of the direct translocation mechanism, four pathways have been implicated: inverted micelles, pore formation, carpet model and membrane-thinning model [12].

As a typical representative of polycationic and arginine-rich CPPs, the human immunodeficiency virus type 1 (HIV-1) TAT peptide is one of the best characterized CPPs [17]. Since the TAT peptide (^{47}YGRKKRRQRRR^{57}) carries a net charge of +8, many previous studies have initially assumed that the efficient internalization of TAT peptide strongly relies on the electrostatic interactions between the positively charged arginine residues of peptide and the negatively charged headgroups of phospholipid like phosphoserine and phosphoglycerol [18-20]. However, such a proposal does have two obvious weaknesses: 1) Anionic phospholipids are minor constituent of the eukaryotic cell membrane and few (~2%) are present on the external leaflet of the plasma membrane [21] , 2) Arginine-rich CPPs have much better internalization capacity than other polycationic CPPs, such as lysine- and histidine -rich peptides [4,22]. These evidences clearly indicate that the electrostatic attraction alone is insufficient for the internalization of TAT peptide. Indeed, a growing number of studies have turned to another explanation that the bidentate hydrogen bonds formed between the guanidinium ions on arginine residues and the phosphate moieties on lipid headgroups might play a unique role in facilitating the translocation of TAT peptide [19,22-25]. With the aim of clarifying the exact contribution of electrostatic attraction in the internalization of TAT peptide, this paper reports the use of a sensitive method –neutron lamellar diffraction – to determine the unambiguous distributions of TAT peptides across the neutral DOPC bilayer.

In our previous neutron diffraction experiments, the distribution of TAT peptides in a partially negatively-charged phospholipid bilayer (DOPC/DOPS) was investigated, and two populations of peptide, in the glycerol backbone region of bilayer and the peripheral water phase between adjacent bilayers, were established [26]. We believed the intrinsic deep-insertion of TAT peptide in the hydrophobic core region of the lipid bilayer was largely repelled by the strong electrostatic attractions between the negatively-charged headgroups of phospholipid and the positively charged TAT peptides. It subsequently leads us to speculate the role that the negatively-charged headgroups of DOPS lipid play in the internalization of TAT peptide may be less important than previously thought [26]. In present study, we extend our first experiment, and focus on whether the TAT peptides can insert into the pure neutral DOPC lipid bilayer. The distribution of TAT peptides in the DOPC bilayer and the perturbation of water distribution across the bilayer will be revealed.

METHODS

Chemicals

TAT peptide (^{47}YGRKKRRQRRR^{57}) was purchased from Almac Sciences Ltd. (Edinburgh, U.K.). The purity of TAT peptide was higher than 95%, as revealed by HPLC and MALDI-TOF mass spectrometry. 1,2-dioleoyl-sn-glycero-3-phosphocholine (DOPC) was purchased from Avanti Polar Lipids Inc. (USA) and used without further purification. Chloroform and other chemicals were of analytical-reagent grade and purchased from Sigma-Aldrich (U.K.).

Sample Preparation

20 mg of lyophilized DOPC lipids were first dissolved in chloroform as a lipid stock solution. TAT peptide was dissolved in ultrapure water (Merck Millipore) and then mixed with the DOPC lipid stock solution to form desired peptide-to-lipid molar ratios (P/L) of 1 to 10 %. To ensure the peptide and DOPC lipid were mixed uniformly, the mixtures were vortexed vigorously for 10 minutes. Finally, the mixtures were deposited onto quartz microscope slides (75 mm x 25 mm) by an artist's airbrush, utilizing nitrogen as a propellant. Solvents were removed under vacuum for over 6 hours.

Neutron Diffraction data collection and analysis

Neutron diffraction data were collected on the D16 instrument at the Institut Laue-Langevin (ILL), France, using the real-time swelling-series method as previously described [27, 28]. Dried lipid mixtures were re-hydrated at various relative humidities using saturated salt solutions of KCl, KNO_3 or K_2SO_4 in 8.06% or 25% (v/v) ^2H_2O. The saturated salt solutions set the relative humidity to 84%, 94% or 98%, respectively. The sample was kept in a sealed aluminum chamber at 25°C for over 6 hours in order to reach equilibrium. The slide with fully equilibrated lipid sample was rapidly mounted on a goniometer of the diffractometer for measurement. The wavelength of neutrons was 4.740 Å. The diffraction data collection and analysis procedure for all the lipid samples are the same as previously described [26].

RESULTS

Structure factors and scattering length density profiles

A series of measurements were conducted to compare the distributions of TAT peptides across the DOPC bilayer at various peptide concentrations from 1 to 10 mol%, following the real-time swelling-series protocol. (See supplemental material for raw diffraction data). At the isotopic composition of 8.06% ^2H_2O, the negative scattering of hydrogen nuclei is exactly balanced by the positive scattering of oxygen and deuterium nuclei, meaning that the neutron scattering by water is eliminated (zero). The distinct advantage of this special condition is that all observed structure factors from various experiments can lie on the same continuous transform, thereby allowing a same function to be fitted simultaneously to all observed points. Compared to the $^2H_2O/H_2O$ exchange method, the requirement for scaling between measurements in the same series disappears and the accuracy of intensity measurement is much improved [28].

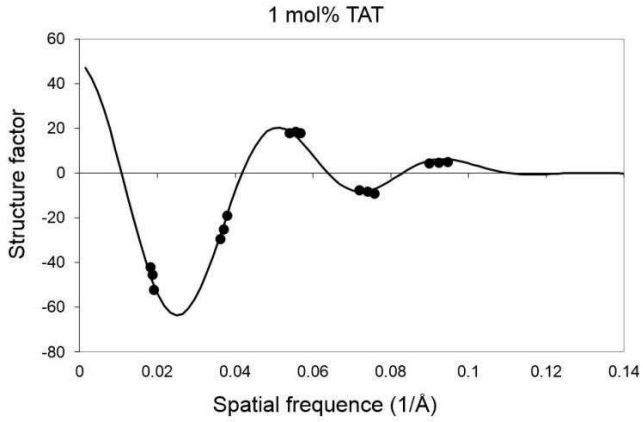

Figure 1. Demonstration of the phase determination of structure factors. The solid points are the

corrected but unscaled structure factors at 3 different relative humidities, and the line is a fit of a continuous transform for phase determination (- - + - + for orders 1–5 in the DOPC lipid bilayer with 1 mol% of TAT peptide).

To help phase the diffraction data, and obtain more detailed structural information, the lamellar *D*-repeat was systematically varied by changing the membrane hydration. Figure 1 illustrates how the data were fitted to assign phases to structure factors derived from diffraction peak intensities. Experimentally determined structure factors for 5 orders at 3 different relative humidities were plotted in reciprocal space and assigned positive or negative values to achieve a least-squares minimization, subsequently satisfying the Shannon's sampling theorem [27-29]. Table 1 summarizes all the experimentally derived and phased structure factors used to reconstruct the scattering length density (SLD) profiles in presence and absence of TAT peptide with 8.06 % ^2H_2O, including the form factor errors from the fitting procedure. The phased structure factors were then placed on a relative absolute scale to reconstruct the SLD profile by Fourier synthesis, following the procedure previously described [27,28]. The observed difference profile (red broken line) was fitted as two Gaussian shaped peaks in reciprocal space, revealing the position, width and area of the transbilayer peptide distribution, as seen in Figure 2. The blue solid line is a fit of two Gaussian functions to the difference profile, whose parameters are summarized in Table 3.

P/L ratio	*F(1)*	*F(2)*	*F(3)*	*F(4)*	*F(5)*
0%	-42.06 ± 0.36	-25.46 ± 0.18	17.59 ± 0.15	-8.48 ± 0.07	4.03 ± 0.03
1%	-46.38 ± 0.23	-25.33 ± 0.12	17.48 ± 0.18	-8.26 ± 0.04	6.01 ± 0.06
3%	-45.94 ± 0.32	-23.01 ± 0.21	16.15 ± 0.09	-10.41 ± 0.07	5.48 ± 0.01
5%	-38.65 ± 0.28	-16.69 ± 0.16	12.02 ± 0.12	-6.16 ± 0.04	4.50 ± 0.03
10%	-51.38 ± 0.45	-16.09 ± 0.12	9.89 ± 0.08	-5.47 ± 0.05	6.41 ± 0.08

Table 1. Experimental determined and phased structure factors of DOPC lipid bilayers in presence and absence of different concentrations of TAT peptide, with 8.06 % ^2H_2O.

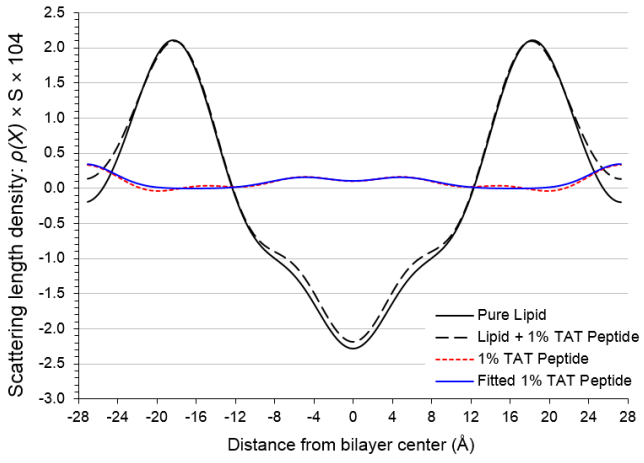

2A

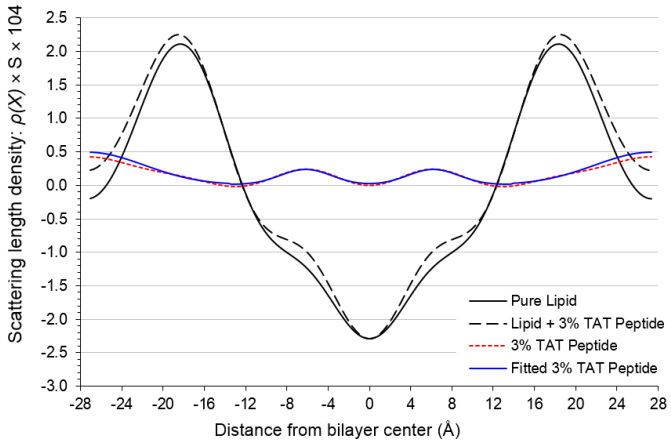

2B

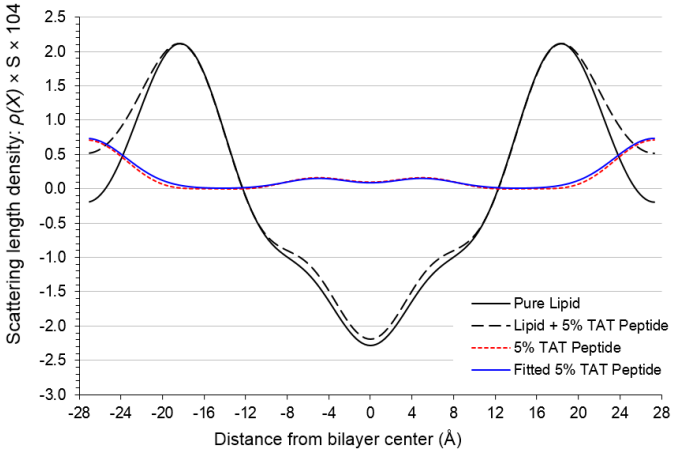

2C

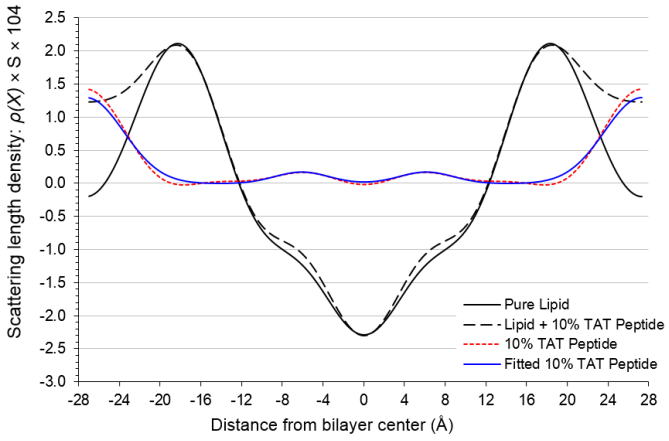

2D

Figure 2. Neutron scattering length density profiles of a pure DOPC lipid bilayer (black solid line), of lipid bilayers with different amount of TAT peptide (black broken line) at 8.06% $^{2}H_2O$, and a difference profile calculated by subtracting structure factors for pure lipid from structure factors for lipid with TAT peptide (red broken line) are displayed. A fit of two Gaussian functions to the difference profile was to determine the position, width and area of peptide distribution (blue solid line). From Figure 2A to 2D, the amount of TAT peptide increased.

D-repeat and bilayer thickness

The lamellar *D*-repeat of the pure DOPC bilayer, calculated using the Bragg equation from 5 orders

of diffraction at a relative humidity of 98%, was 53.9 Å (Table 2). When more peptides up to 5 mol% were introduced, no significant change was found in *D*-repeat. A huge increase of 2.8 Å was only observed at 10 mol% peptide concentration, compared to the pure DOPC lipid (56.7 vs 53.9 Å). The bilayer thickness was extracted from the SLD profile of the bilayer at 8.06% $^{2}H_2O$ (Figure 2), which is defined as the distance between the two maxima in the SLD profile. Values for the putative bilayer hydrophobic thickness are presented in Table 2. When 1 mol% peptide was firstly introduced into the bilayer, the bilayer thickness immediately shrank from 36.6 to 35.6 Å. No significant bilayer thinning was detected, when the peptide concentration was further increased up to 10 mol%.

P/L ratio	0%	1%	3%	5%	10%
D-repeat (Å)	53.9	54.1	54.2	53.9	56.7
Bilayer thickness (Å)	36.6	35.6	35.5	35.5	35.5

Table 2. *D*-repeat and putative bilayer thickness of DOPC lipid bilayer in presence and absence of TAT peptide at 98%RH, with 8.06 % $^{2}H_2O$.

Peptide distribution in DOPC lipid bilayer

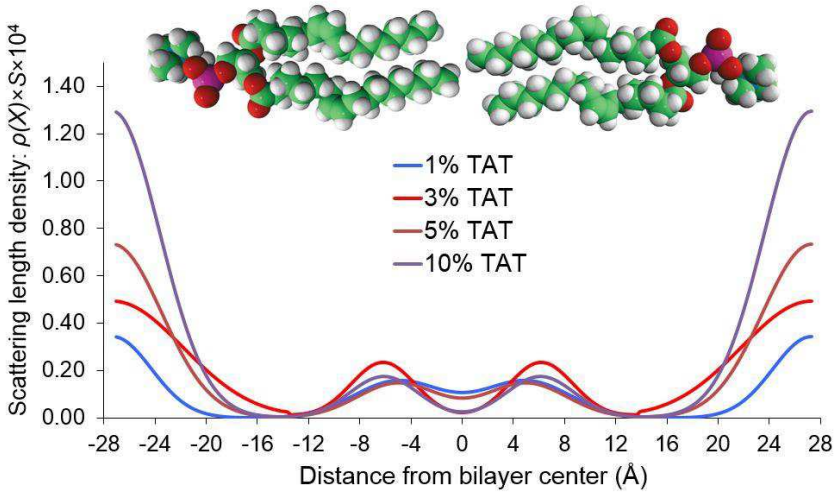

Figure 3. Summary of the Gaussian fits to observed peptide (difference SLD) profiles at a series of peptide concentrations, representing TAT peptide distributions in neutral DOPC bilayers. The interbilayer water compartment is at the two edges of the graph. A pair of phospholipid molecules is shown above the graph to illustrate the orientation of the lipid bilayer. The comparison is set to the same *D*-repeat.

TAT peptide distribution		L/P=100:1	L/P=100:3	L/P=100:5	L/P=100:10
Gaussian 1	Position (Å)	27.3	27.3	27.3	27.3
	Width (Å)	4.3	7.8	5.4	5.2
	Occupancy (%)	49.1	69.7	75.1	83.6
Gaussian 2	Position (Å)	5.0	6.2	5.0	6.1

	Width (Å)	4.9	3.5	4.5	3.8
	Occupancy (%)	50.9	30.3	24.9	16.4

Table 3. Summary of the Gaussian fit parameters for the calculated peptide (difference SLD) profiles in reciprocal space. Five orders of diffraction were used in the fitting procedure. The position of TAT peptide is expressed as the distance from the center of the bilayer. The width is the full width at half height.

As seen in Figure 3 and Table 3, the best fit to the observed peptide profile shows that the interactions between TAT peptides and a neutral DOPC lipid bilayer took place at two discrete positions. One involved deep insertion into the bilayer core region a depth of 6.0 Å from the center of the bilayer, a position close to the double bond of the fatty acyl chain. While the second one was more peripheral at a depth of 27.3 Å from the center of the bilayer, the edge of centrosymmetric unit cell, representing the aqueous bulk between adjacent bilayers. When the TAT peptide concentration increased from 1 to 10 mol%, the positions of two peptide populations across the bilayer did not shift. Interestingly, the population increase could only be observed in the peripheral aqueous phase between adjacent bilayers but not in the hydrophobic core region of the bilayer, upon the introduction of more peptides into the bilayer (Figure 3). This change was found to be highly proportional to the molar ratio of peptide introduced (R^2=0.90, data not shown).

Water distribution in DOPC lipid bilayer

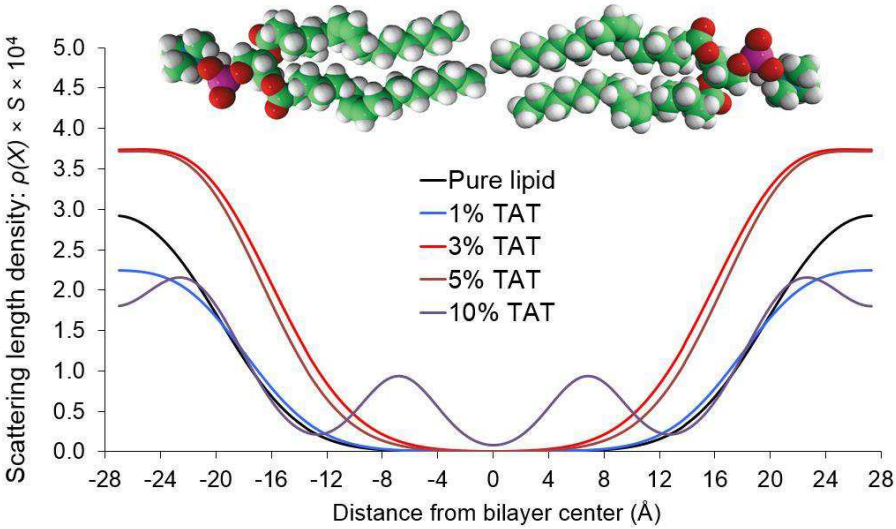

Figure 4. Summary of Gaussian fitting results to observed water (difference SLD) profiles at a series of TAT peptide concentrations in neutral DOPC bilayers. The interbilayer water compartment is at the two edges of the graph. A pair of phospholipid molecules is shown above the graph to illustrate the orientation of the lipid bilayer. All comparisons are set on the same *D*-repeat.

Water distribution		Pure Lipid	L/P=100:1	L/P=100:3	L/P=100:5	L/P=100:10
Gaussian 1	Position	23.5	22.5	21.7	21.4	22.2
	Width (Å)	7.2	7.2	7.5	7.8	5.6
	Occupancy	100	100	100	100	76.2

Gaussian 2	Position	-	-	-		6.8
	Width (Å)	-	-	-		3.9
	Occupancy	-	-	-		23.8

Table 4. Summary of the parameters of fitting Gaussian distribution to the calculated water (difference SLD) profiles in reciprocal space. Five orders of diffraction were used in the fitting procedure. The position of water is expressed as the distance from the center of the bilayer. The width is the full width at half height.

The water distribution across the bilayer provided additional support to the interaction of TAT peptides with a DOPC lipid bilayer. The observed water profiles were calculated by subtracting the structure factors at 8.06% $^{2}H_2O$ from those at 25% $^{2}H_2O$. All fitted water profiles are compared in Figure 4 and the resultant parameters from the Gaussian fitting are summarized in Table 4. Increasing amount of water is seen in Figure 4, where the water distribution grows in width and moves toward the center of the bilayer when more peptides are introduced (1 to 5 mol%). This suggests more water molecules were needed to maintain the TAT peptides hydrated, when more peptides occupied a deeper position of the bilayer. However, no water penetrates into the hydrophobic core region of the DOPC lipid bilayer, as the water density in the center of the bilayer is marginal at all peptide concentrations lower than 10 mol%.

A significant change on the water profile was found at the highest peptide concentration investigated (10 mol%). The best fit to this water profile can only be modeled by two discrete Gaussian peaks, representing two water populations across the bilayer. 24% of water population deeply intercalated into the glycerol backbone region at a depth of 6.8 Å from the center of the bilayer, a position close to the double bonds of the oleoyl acyl chain, while 76% of water population kept in the aqueous bulk between adjacent bilayers at a depth of 22.2 Å from the center of the bilayer. As the width of the deep intercalated water distribution (3.9 Å) covers almost the entire hydrophobic core region of the bilayer, it is very clear evidence that a transbilayer water pore was formed at the highest peptide concentration investigated (10 mol%).

DISCUSSION

Our neutron diffraction data clearly shows that the interactions of TAT peptides with a neutral DOPC lipid bilayer were varied in a concentration-dependent manner. The bilayer thickness significantly shrank and water densities greatly shifted when 1 mol% peptide was firstly introduced into the bilayer. No obvious bilayer thinning and water moving toward the bilayer core were detected, when the peptide concentration was further increased up to 5 mol%. A significant structure distortion – a transbilayer water pore – was only found at the highest peptide concentration investigated (10 mol%). In fact, similar water defect formations have been implicated by previous MD simulation studies. MacCallum's group demonstrated that the translocation of an arginine across the pure DOPC bilayer accompanied by the formation of a water defect that keeps the arginine hydrated even at the center of the bilayer [30]. Li and his colleagues showed that any attempt to hold the location of a single charged arginine deeper in the bilayer than its free energy location would severely distort the pure DPPC bilayer by opening a hole above it that will draw in water [31]. Furthermore, it was demonstrated that octa-arginine (R8) peptides interacted with each other in a cooperative manner to

prolong the life-time of transient pores presented in the DPPC bilayer, thereby facilitating the rapid translocation of peptides. When a threshold concentration of octa-arginine peptide in the bilayer was reached，a steady-state water pore would form [25].

It should be noted that the neutron diffraction form factors measure an equilibrium state of lipid bilayer samples [27,28]. If the form factors obtained from experiments were agreed with a water pore structure, it would indicate that the pore structure in the bilayer was at steady state and not transient. Conversely, any non-equilibrium structure like a transient water defect which has been constantly implicated by other studies could not be extracted from the neutron diffraction method. Although the water defect formations by drawing lipid headgroups and water molecules into the bilayer core is partially supported by the bilayer thinning and the water densities moving towards the center of the bilayer observed in our experiments.

Similar concentration-dependent behaviors of the arginine-rich peptides have been described by other studies [25,32]. A critical peptide concentration was needed for a water pore formation when hexa-arginine peptides interacted with a DMPC/DMPS anionic lipid bilayer [32]. Another intriguing study reported that the translocation of arginine molecules into the DOPC lipid bilayer is highly nonadditive [30]. Once a water defect was formed and the free energy penalty had been paid by the first arginine, relatively small free energy was required to transfer additional arginine molecules into the existing water defect. No significant change would be expected from the distribution of water or lipid headgroups [30]. All above early findings are in good agreement with our current observations.

The driving force of direct membrane translocation

Like most of the early studies on polycationic CPPs, we had initially assumed that the strong electrostatic attractions between the positively charged TAT peptides and the negatively charged headgroups of phospholipid are the key factor for the translocation of TAT peptide [18,33]. The interactions of TAT peptides with a negatively charged DOPC/DOPS lipid bilayer were previously investigated using the neutron diffraction, when two populations of the TAT peptide across the anionic lipid bilayer were detected [26]. One is in the peripheral aqueous phase between adjacent bilayers at 25 Å and the other is below the glycerol backbone region at a depth of 14 Å from the center of the bilayer, under all peptide concentrations investigated (from 0.1 to 10 mol%). Most notably, at the highest peptide concentration investigated (10 mol%), no deep insertion of TAT peptide into the hydrophobic core region of the DOPC/DOPS bilayer was found and most of peptides were still constrained on the glycerol backbone region of bilayer [26]. We proposed that the negatively charged headgroups of lipid bilayer prevented the TAT peptides from their intrinsic intercalation into the hydrophobic core region of the bilayer, leading to more surface distribution of peptides in the peripheral aqueous phase of the bilayer and diminished translocation efficiency. It has prompted us to speculate the role that the electrostatic attractions between the negatively charged headgroups of phospholipid and the positively charged TAT peptides play in the translocation of TAT peptide may be less important than previously thought.

The above argument is convincingly supported by our current data where the TAT peptides deeply intercalated into the hydrophobic core region of a neutral DOPC lipid bilayer at a depth of 6.0 Å from the center of the bilayer, a position close to the double bond of the fatty acyl chain. Obviously,

the TAT peptide can intercalate into a much deeper position in the bilayer, without the negatively charged phospholipids. This notion is well corroborated by other previous studies using different techniques. A very recent work using X-ray scattering showed that the bilayer thinning and the disruption of acyl chains were observed when the TAT peptides interacted with a neutral DOPC lipid bilayer, and such bilayer deformations were not affected by the increasing DOPE lipid content [(34)]. An atomic force microscopy work showed that the TAT peptide can bind to a neutral DOPC/SM/cholesterol mixture lipid bilayer without any negatively charged lipids [(35)]. A solid-state ^{31}P NMR spectroscopy study demonstrated that the TAT peptide only induced pronounced isotropic lipid morphology in a pure neutral DMPC lipid bilayer, but not in a pure anionic DMPG lipid bilayer. The isotropic signal of lipid morphology significantly decreased when the anionic DMPG lipid content increased [(36)]. Therefore, we conclude that the electrostatic attractions between the positively charged TAT peptides and the negatively charged headgroups of phospholipid are not a prerequisite for the direct membrane translocation. As many previous studies have demonstrated that the internalization of CPPs might occur through distinct pathways in the same time, including direct translocation and endocytosis [(13,14)], we do not preclude the potential role of the electrostatic attractions plays in the initiation of endocytosis pathway. In fact, we suggest such electrostatic interaction on the surface of lipid bilayer might function as a switch to control the different internalization mechanisms of CPPs under various physiological conditions.

Concerning the basic driving force of the membrane translocation of TAT peptide, accumulating studies are leading to a more reasonable explanation that the multidentate hydrogen bonds formed between the guanidinium ions on arginine residues and the phosphate moieties on lipid headgroups play a unique role in facilitating the translocation of TAT peptide [(19,22-25)]. A previous MD simulation study demonstrated that the like-charge ion pairing was found to shape when transferring guanidinium ions inside a POPC lipid bilayer, thereby leading to transient pore formations [(23)]. They concluded that the guanidinium ion pairing was the key factor that facilitates the highly charged peptide to compress inside the membrane defect without affecting the membrane integrity. This seems to be supported by our observation that no severe distortion of bilayer was found under the low peptide concentrations investigated (1 to 5 mol%).

The insertion of TAT peptide in the hydrophobic core region of lipid bilayer

From the conventional view based on the continuum electrostatic model, the translocation of charged molecules from an aqueous solution to a low dielectric lipid membrane is strongly disfavored. Our observation that the deep intercalation of a highly positively charged TAT peptide (carrying a net charge of +8) in the hydrophobic core region of lipid bilayer is opposing the prevailing view in membrane biophysics. An intriguing question is raised by our surprising observation that whether the charged amino acids like arginine can remain in a low dielectric lipid hydrocarbon environment. This question was highlighted by the recent model of voltage-gated ion channel which utilizes the arginine side chains to detect transmembrane voltage changes [(37,38)] and the active membrane translocation of arginine-rich CPPs [(22-25)]. If the interactions between arginine molecules and a membrane bilayer are governed by a Born-type free energy model, the cost of transferring an arginine from the water to the membrane center should be as high as ~170 kJ/mol [(39)]. However, the lipid membrane is a flexible and dynamic structure which should not be simply treated as rigid slabs of hydrocarbon. The ion-membrane interactions cannot be simply described by the continuum

electrostatic model. In fact, MD simulations from several groups have found that the free energy cost for placing an arginine into the bilayer core is ~60 to 80 kJ/mol, which is much smaller than traditionally thought [30,39,40]. Intriguingly, a water defect structure in the bilayer was adopted to maintain the arginine residues hydrated by drawing water molecules and lipid headgroups into the bilayer core, when transferring an arginine across the bilayer. There were one lipid headgroup and four or five water molecules coordinated with an arginine [30,31]. This seems to be supported by the thinning of DOPC bilayer under low peptide concentrations investigated (1 to 5 mol%) and the presence of transbilayer water pore at the highest peptide concentration investigated (10 mol%) from our observations. Therefore, the free energy costs for transferring an arginine across the bilayer are not only associated with dehydration, but also associated with the bilayer deformations to maintain the arginine molecule hydrated. Without bilayer deformations, the free energy costs will be doubled, which would lead to a complete deprotonation of arginine [41].

Moreover, biological membranes are composed of many different types of lipid, carbohydrate, and protein - along with an asymmetric distribution of lipids between membrane leaflets, the energy to overcome the dielectric barrier could differ substantially depending on the exact composition of the membrane. Accumulating evidences are showing that the introduction of nonopolar amino acids, helical proteins and specific lipid molecules into the biological membrane will provide additional stabilization to water defects and further lower the free energy cost [31,41,42]. It is reasonable to argue that the free energy cost of ~ 60 kJ/mol for transferring an arginine into the bilayer core from current experimental and computational studies is still overestimated for the passive diffusion of arginine-rich CPPs in a biological - rather than model - membrane. In short, all above evidences suggested that considerably less free energy is required to place the arginine residues in the center of the bilayer than might be expected. This hypothesis would confidently satisfy our observation that the deep intercalation of TAT peptides into the hydrophobic core region of DOPC bilayer and bring important implications for the efficient membrane translocation of arginine-rich and polycationic CPPs.

CONCLUSIONS

In summary, the study presented here was completed by using the neutron lamellar diffraction method to investigate the interactions between TAT peptides and a neutral DOPC lipid bilayer. When compared to our previous study on an anionic DOPC/DOPS lipid bilayer, much deeper intercalation of TAT peptide was found in the hydrophobic core region of the neutral DOPC lipid bilayer at a depth of 6.0 Å from the center of the bilayer, a position close to the double bond of fatty acyl chain. These observations lead to an unambiguous conclusion that the electrostatic attractions between the positively charged TAT peptides and the negatively charged headgroups of phospholipid like phosphoserine are not a prerequisite for the efficient translocation of TAT peptide.

Moreover, we propose a mechanism of the translocation of TAT peptide across the neutral DOPC lipid bilayer. A limited number of peptides first associate with the phosphate moieties on the lipid headgroups by using the guanidinium ions pairing. Then the energetically favorable water defect structures are adopted to maintain the arginine residues hydrated by drawing water molecules and lipid headgroups into the bilayer core. Such bilayer deformations consequently lead to the deep intercalation of TAT peptides into the bilayer core at a depth of 6.0 Å from the center of the bilayer, a

position close to the double bond of fatty acyl chain. Once a threshold concentration of TAT peptide in the bilayer is reached, a significant rearrangement of lipid bilayer will happen and steady-state water pores will form.

Our findings show that the lipid composition and the peptide concentration present can cast a profound effect on the direct translocation of TAT peptide. Understanding the mechanism by which arginine-rich CPPs interact with the lipid bilayer will greatly contribute to our fundamental knowledge of the mechanism behind internalization of charged molecules through the cell membrane, and the design of more efficient transporters for bioactive drug delivery.

AUTHOR CONTRIBUTIONS

X.C., S.L., P.R., and J.B. designed the experiments. X.C., V.C. B.D. and Y.W. performed the experiments and analyzed the data. X.C., D.M. R.W. and J.B participated in writing and editing the manuscript.

ACKNOWLEDGMENTS

This work was supported by grants from Overseas Research Scholarship from The University of Edinburgh (UK), the Institut Laue-Langevin (France) and Canadian Neutron Beam Centre (Chalk River). This work has been funded in part by the Natural Science Foundation of Fujian Province (China) under grant no. 2015J01134 and the Natural Science Foundation of Education Department of Fujian Province (China) under grant no. JA15062. Special thanks to Alastair. A. Macdonald, who kindly helped proofread the manuscript.

REFERENCES

1. C. Bechara, S. Sagan, Cell-penetrating peptides: 20years later, where do we stand?, FEBS Letters. 587 (2013) 1693–1702.
2. E. Koren, V.P. Torchilin, Cell-penetrating peptides: breaking through to the other side, Trends in Molecular Medicine. 18 (2012) 385–393.
3. V.P. Torchilin, Tat peptide-mediated intracellular delivery of pharmaceutical nanocarriers, Advanced Drug Delivery Reviews. 60 (2008) 548–558.
4. E. Vivès, J. Schmidt, A. Pèlegrin, Cell-penetrating and cell-targeting peptides in drug delivery, Biochimica Et Biophysica Acta (BBA) - Reviews on Cancer. 1786 (2008) 126–138.
5. S.B. Fonseca, M.P. Pereira, S.O. Kelley, Recent advances in the use of cell-penetrating peptides for medical and biological applications☆, Advanced Drug Delivery Reviews. 61 (2009) 953–964.
6. N.A. Brooks, D.S. Pouniotis, C.-K. Tang, V. Apostolopoulos, G.A. Pietersz, Cell-penetrating peptides: Application in vaccine delivery, Biochimica Biophysica Acta - Reviews on Cancer. 1805 (2010) 25–34.
7. S.M. Farkhani, A. Valizadeh, H. Karami, S. Mohammadi, N. Sohrabi, F. Badrzadeh, Cell penetrating peptides: Efficient vectors for delivery of nanoparticles, nanocarriers, therapeutic and diagnostic molecules, Peptides. 57 (2014) 78–94.
8. S. Jafari, S.M. Dizaj, K. Adibkia, Cell-penetrating peptides and their analogues as novel

nanocarriers for drug delivery, Bioimpacts. 5 (2015) 103–111.

9. F. Milletti, Cell-penetrating peptides: classes, origin, and current landscape, Drug Discovery Today. 17 (2012) 850–860.
10. M.D. Pisa, G. Chassaing, J.-M. Swiecicki, Translocation Mechanism(s) of Cell-Penetrating Peptides: Biophysical Studies Using Artificial Membrane Bilayers, Biochemistry. 54 (2015) 194–207.
11. M. Zorko, U. Langel, Cell-penetrating peptides: mechanism and kinetics of cargo delivery, Advanced Drug Delivery Reviews. 57 (2005) 529–545.
12. F. Madani, S. Lindberg, Ü. Langel, S. Futaki, A. Gräslund, Mechanisms of Cellular Uptake of Cell-Penetrating Peptides, Journal of Biophysics. 2011 (2011) 1–10.
13. R. Brock, The Uptake of Arginine-Rich Cell-Penetrating Peptides: Putting the Puzzle Together, Bioconjugate Chem. Bioconjugate Chemistry. 25 (2014) 863–868.
14. N. Ben-Dov, R. Korenstein, The uptake of HIV Tat peptide proceeds via two pathways which differ from macropinocytosis, Biochimica Et Biophysica Acta (BBA) - Biomembranes. 1848 (2015) 869–877.
15. F. Heitz, M.C. Morris, G. Divita, Twenty years of cell-penetrating peptides: from molecular mechanisms to therapeutics, British Journal of Pharmacology. 157 (2009) 195–206.
16. A. Walrant, L. Matheron, S. Cribier, S. Chaignepain, M.-L. Jobin, S. Sagan, et al., Direct translocation of cell-penetrating peptides in liposomes: A combined mass spectrometry quantification and fluorescence detection study, Analytical Biochemistry. 438 (2013) 1–10.
17. D.M. Copolovici, K. Langel, E. Eriste, Ü. Langel, Cell-Penetrating Peptides: Design, Synthesis, and Applications, ACS Nano. 8 (2014) 1972–1994.
18. H.D. Herce, A.E. Garcia, Molecular dynamics simulations suggest a mechanism for translocation of the HIV-1 TAT peptide across lipid membranes, Proceedings of the National Academy of Sciences. 104 (2007) 20805–20810.
19. J.B. Rothbard, T.C. Jessop, R.S. Lewis, B.A. Murray, P.A. Wender, Role of Membrane Potential and Hydrogen Bonding in the Mechanism of Translocation of Guanidinium-Rich Peptides into Cells, J. Am. Chem. Soc. Journal of the American Chemical Society. 126 (2004) 9506–9507.
20. M.-L. Jobin, I.D. Alves, On the importance of electrostatic interactions between cell penetrating peptides and membranes: A pathway toward tumor cell selectivity?, Biochimie. 107 (2014) 154–159.
21. M.-L. Jobin, M. Blanchet, S. Henry, S. Chaignepain, C. Manigand, S. Castano, et al., The role of tryptophans on the cellular uptake and membrane interaction of arginine-rich cell penetrating peptides, Biochimica Et Biophysica Acta (BBA) - Biomembranes. 1848 (2015) 593–602.
22. A. Mishra, V.D. Gordon, L. Yang, R. Coridan, G.C.L. Wong, HIV TAT Forms Pores in Membranes by Inducing Saddle-Splay Curvature: Potential Role of Bidentate Hydrogen Bonding, Angewandte Chemie Angew. Chem. 120 (2008) 3028–3031.
23. C. Allolio, K. Baxova, M. Vazdar, P. Jungwirth, Guanidinium Pairing Facilitates Membrane Translocation, The Journal of Physical Chemistry B J. Phys. Chem. B. 120 (2016) 143–153.
24. M. Vazdar, J. Vymětal, J. Heyda, J. Vondrášek, P. Jungwirth, Like-Charge Guanidinium Pairing from Molecular Dynamics and Ab Initio Calculations, J. Phys. Chem. A The Journal of Physical Chemistry A. 115 (2011) 11193–11201.
25. D. Sun, J. Forsman, M. Lund, C.E. Woodward, Effect of arginine-rich cell penetrating peptides

on membrane pore formation and life-times: a molecular simulation study, Phys. Chem. Chem. Phys. 16 (2014) 20785–20795.

26. X. Chen, F. Sa'adedin, B. Deme, P. Rao, J. Bradshaw, Insertion of TAT peptide and perturbation of negatively charged model phospholipid bilayer revealed by neutron diffraction, Biochimica Biophysica Acta - Biomembranes. 1828 (2013) 1982–1988.
27. J.P. Bradshaw, M.J. Darkes, S.M. Davies, Improved accuracy and phasing of lamellar neutron diffraction data by real-time swelling series method, Physica B: Condensed Matter. 241-243 (1997) 1115–1121
28. M.J.M. Darkes, J.P. Bradshaw, Real-time swelling-series method improves the accuracy of lamellar neutron-diffraction data, Acta Crystallogr D Biol Crystallogr.. 56 (2000) 48–54.
29. M.J. Darkes, T. Hauss, S. Dante, J.P. Bradshaw, Revealing the membrane-bound structure of neurokinin A using neutron diffraction, Physica B: Condensed Matter. 276-278 (2000) 505–507.
30. J.L. MacCallum, W.D. Bennett, D.P. Tieleman, Transfer of arginine into lipid bilayers is nonadditive, Biophysical Journal 101 (1) (2011)110117.
31. L. Li, I. Vorobyov, A.D. Mackerell, T.W. Allen, Is Arginine Charged in a Membrane?, Biophysical Journal. 94 (2008). L11–L13
32. J.-M. Hu, W.-D. Tian, Y.-Q. Ma, Computational Investigations of Arginine-Rich Peptides Interacting with Lipid Membranes, Macromolecular Theory and Simulations Macromol. Theory Simul. 24 (2015) 399–406.
33. Y. Su, A.J. Waring, P. Ruchala, M. Hong, Membrane-Bound Dynamic Structure of an Arginine-Rich Cell-Penetrating Peptide, the Protein Transduction Domain of HIV TAT, from Solid-State NMR, Biochemistry. 49 (2010) 6009–6020.
34. K. Akabori, K. Huang, B.W. Treece, M.S. Jablin, B. Maranville, A. Woll, et al., HIV-1 Tat membrane interactions probed using X-ray and neutron scattering, CD spectroscopy and MD simulations, Biochimica Et Biophysica Acta (BBA) - Biomembranes. 1838 (2014) 3078–3087.
35. J.E. Shaw, R.F. Epand, J.C. Hsu, G.C. Mo, R.M. Epand, C.M. Yip, Cationic peptide-induced remodelling of model membranes: Direct visualization by in situ atomic force microscopy, Journal of Structural Biology. 162 (2008) 121–138.
36. S. Afonin, A. Frey, S. Bayerl, D. Fischer, P. Wadhwani, S. Weinkauf, et al., The Cell-Penetrating Peptide TAT(48-60) Induces a Non-Lamellar Phase in DMPC Membranes, ChemPhysChem. 7 (2006) 2134–2142.
37. L. Li, I. Vorobyov, T.W. Allen, Potential of mean force and pKa profile calculation for a lipid membrane exposed arginine side chain, Journal of Physical Chemistry B. 112 (2008) 9574-9587.
38. D. Krepkiy, M. Mihailescu, K. J. Swartz. Structure and hydration of membranes embedded with voltage-sensing domains. Nature. 462(2009) 473–479.
39. F. Khalili-Araghi, V. Jogini, K. Schulten. Calculation of the gating charge for the Kv1.2 voltage-activated potassium channel. Biophys. J. 98 (2010) 2189–2198.
40. S. Dorairaj, T. W. Allen. On the thermodynamic stability of a charged arginine side chain in a transmembrane helix. Proc. Natl. Acad. Sci. USA. 104 (2007) 4943–4948.
41. J. L. MacCallum, W. F. Bennett, D. P. Tieleman. Distribution of amino acids in a lipid bilayer from computer simulations. Biophys. J. 94 (2008) 3393–3404.
42. J. Yoo, Q. Cui, Does arginine remain protonated in the lipid membrane? Insights from microscopic pK a calculations. Biophys. J. 94 (2008) L61-L63.

Graphical abstract

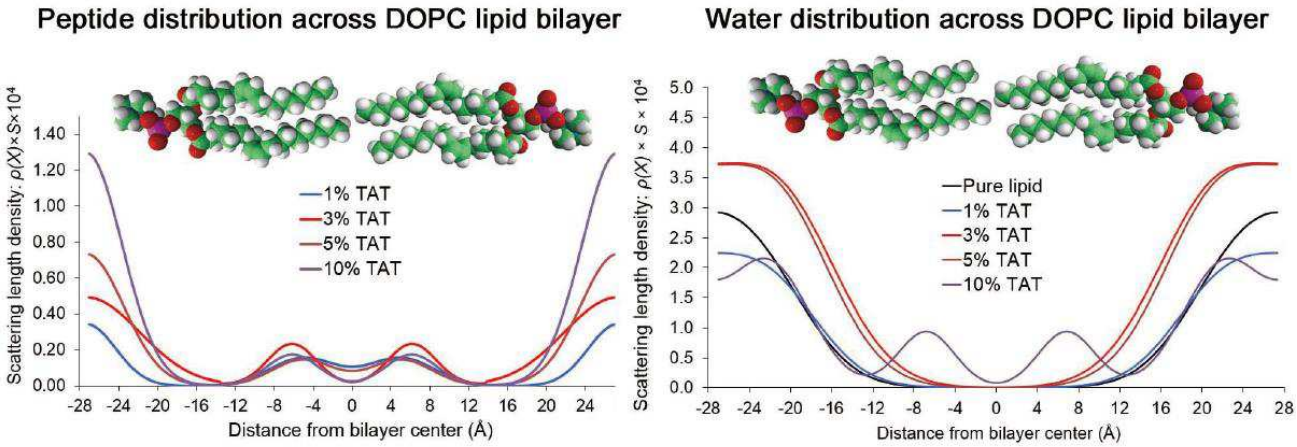

Highlights

- The interactions between TAT peptides and a DOPC lipid bilayer was studied by neutron diffraction.
- TAT peptides was found in the core region of DOPC bilayer at a depth of 6.0 Å from the center of bilayer.
- The interactions were found to vary in a concentration-dependent manner.
- A threshold concentration of TAT peptide in the bilayer is reached, water pores will form.